CrossMark

ORIGINAL PAPER

Investigation of structural parameters and self-aggregation of Algerian asphaltenes in organic solvents

Asma Larbi[1] · Mortada Daaou[1] · Abassia Faraoun[1,2]

Abstract Elemental analysis, Fourier transform infrared (FTIR), ^{1}H-NMR, fluorescence spectroscopy, and surface tension methods have been used to characterize the molecular structure and the aggregation behaviors of two asphaltenic fractions derived, respectively, from an Algerian petroleum well and a corresponding storage tank deposit. Elemental analysis, FTIR, ^{1}H-NMR, and fluorescence spectroscopy were used to investigate the chemical composition and structural parameters of asphaltenes, while the surface tension method was used to measure the critical micelle concentration (CMC) in organic solvents with different solubility parameters and polarities in order to characterize the asphaltenes' aggregation behaviors. Results show that the unstable asphaltenes fraction extracted from the storage tank deposit possesses a higher polarity (higher heteroatoms content) and a lower aromaticity than stable asphaltenes from the petroleum well. The CMC results indicate that asphaltenes with high polarity and low aromaticity have a high solubility in polar solvents such as nitrobenzene, whereas asphaltenes with low polarity and high aromaticity are more soluble in solvents with weak polarity, like toluene. It is concluded that the difference of structure of asphaltene samples and polarity of solvents can lead to difference of aggregation behaviors.

1 Introduction

Asphaltenes constitute the most complex fraction of crude oil. They are conventionally defined as a fraction of crude oil that is insoluble in *n*-alkanes but soluble in toluene. Because of their natural trend to form aggregates that may flocculate and precipitate, asphaltenes can cause severe problems in oil production, transportation, and refining. The propensity of asphaltenes to flocculate is a complex function of the crude oil composition and does not depend directly on the asphaltene content (Kokal and Sayegh 1995). Algerian crude oil is very unstable with respect to aggregation despite the low content of asphaltenes. It is believed that the structural features of asphaltene molecules leading to self-assembly should be taken into account in the study of the probable aggregation mechanism (Yang et al. 2004). According to chemical structure, asphaltenes are aromatic polycyclic molecules surrounded and linked by aliphatic chains and heteroatoms (sulfur, nitrogen, oxygen) as well as traces of metal elements like nickel, iron, and vanadium. The chemical composition and structure of single asphaltene molecules can be assessed using different analytical techniques (Calemma et al. 1995; Shirokoff et al. 1997; Pekerar et al. 1999; Bouhadda et al. 2000; Buenrostro-Gonzalez et al. 2002; Groenzin and Mullins 2000; Ancheyta et al. 2002; Ibrahim et al. 2003; Khan et al. 2003; Avid et al. 2004; Acevedo et al. 2005;

✉ Mortada Daaou
daaou_mortada@yahoo.fr

[1] Laboratoire de Synthèse organique, Physico-chimie, Biomolcules et Environnement (LSPBE), Department of Industrial Organic Chemistry, Faculty of Chemistry, University of Sciences and Technology of Oran, Po. Box 1505, 31000 El-M'naouer, Algeria

[2] Laboratoire de Chimie Physique Macromoléculaire (LCPM), Department of Chemistry, Faculty of Sciences, University of Oran, Po. Box 1524, 31000 El-M'naouer, Algeria

Springer

Siskin et al. 2006). Elemental analysis, mass spectroscopy, and ^{1}H NMR can be used for determination of the average structural parameters such as the aromatic carbon ratio, the average number of alkyl side chains, and the degree of peripheral aromatic carbon substitution (Dereppe et al. 1978; Dickinson 1980; Daaou et al. 2008, 2009).

The polarity and complex structure of asphaltenes can lead to their self-association, flocculation, and precipitation during the course of heavy oil processing. It has been realized that the first step in the formation of precipitated asphaltene particles is the self-aggregation of asphaltenes to form colloidal particles or pseudo-micelles in several solvents. A micelle is a reversible aggregate that is formed in a polar environment and which will remain constant in size and aggregation number for a given set of environmental constraints. Several studies have been carried out employing various methods to determine the "critical micelle concentration" (CMC) of asphaltenes, i.e., the concentration below which asphaltenes remain as monomer species (Taylor 1992). The experimental methods used, including calorimetry (Andersen and Bridi 1991; Andersen and Christensen 2000), surface tension (Sheu 1996; Carbognani et al. 1997; Mohamed et al. 1999; Rogel et al. 2000), viscosity (Storm et al. 1991), vapor pressure osmometry (Yarranton et al. 2000), NIR spectroscopy (Mullins 1990; Kyeongseok et al. 2004), and small-angle scattering measurements (Sheu and Storm 1995) show a variety of the CMC values and indicate that this parameter depends on the asphaltene origin and the solvent used. For instance, Andersen and Bridi (1991) have used microcalorimetric titration for measuring the CMCs of Venezuelan asphaltenes in different organic solvents. They have demonstrated that the breakpoint observed in the curve of the measured enthalpies of the asphaltenes concentrations represents the CMC that might vary from 0.5 to 15 g L^{-1}. Others investigators (Sheu 1996; Bouhadda et al. 2000; Mohamed et al. 1999; Rogel et al. 2000) have employed surface tension measurements to determine the CMC of asphaltenes from different origins in organic solvents. Sheu (1996) has determined the CMC of asphaltenes extracted from Ratawi vacuum residue in pyridine through surface tension measurements, and found a value around 0.4 g L^{-1}. Other surface tension studies have reported that "CMCs of asphaltene in toluene" are much higher, for example, 10 g L^{-1} (Brazilian asphaltenes) in one study (Da Silva Ramos et al. 2001) and 1.7 g L^{-1} (Algerian asphaltenes) in another study (Bouhadda et al. 2000). Rogel et al. (2000) have found that the CMC values of unstable asphaltenes in different solvents, obtained by surface tension measurements, vary in the range of 1–30 g L^{-1}. It is believed that the self-aggregation behavior of asphaltenes is related to the structure and chemical properties of asphaltenes, and by analogy, related

to the behavior of surfactants in aqueous and non-aqueous solutions. On the other hand, some reports have indicated that structure and characteristics of asphaltenes are some of the main factors that determine their relative stability in crude oils (Carbognani et al. 1997). The intermolecular forces including electrostatic interactions, van der Waals forces, intermolecular charge transfer, exchange–repulsion interaction, induction effects, hydrogen bonding, and the so-called π–π interactions are found to be responsible for the asphaltenes aggregation (Murgich et al. 1996; Murgich 2002).

The purpose of this work is comparing structural properties and the aggregation behavior of two asphaltene fractions extracted from two different sources of Algerian petroleum. The first was obtained from the crude oil of the Hassi-Messaoud field. The second fraction was obtained from the oil storage tank deposit formed after the usual treatment (separation of water, salts, and mineral sediments) and pipeline transportation. The physical characteristics of the crude oil and the storage oils are summarized in Table 1.

The structural parameters of both asphaltene fractions were investigated using elemental analysis, Fourier transform infrared (FTIR), H-NMR, and fluorescence spectroscopy. The asphaltene aggregation was assessed determining the CMC in three solvents (toluene, pyridine, and nitrobenzene) with different solubility parameters and polarity using surface tension method.

2 Materials and methods

Two asphaltene samples from Hassi-Messaoud petroleum in Algeria were investigated. The first (AS)$_{DP}$ was extracted from the storage tank deposit, while the second (AS)$_{WL}$ was derived from a Hassi-Messaoud oil well. The toluene, pyridine, and nitrobenzene were from Fisher Chemicals with 99 % purity, while the n-heptane was from Prolabo Chemicals.

The asphaltenes were extracted by addition to petroleum or deposit an excess of n-heptane in 40:1 (volume: mass) ratio. The mixture was subjected to 24 h constant, gentle shaking to ensure complete dispersion of the material. The precipitated asphaltene was then removed by vacuum filtration through a 0.45 μm pore size membrane. The solid obtained was thoroughly washed with n-heptane to remove co-precipitated maltenes until the washing solvent was colorless.

Fourier transform infrared spectra were collected with a Fourier transform IR spectrometer (Spectrum one, Perkin-Elmer) coupled with attenuated total reflectance module (ATR) with a spectral resolution of 4 cm^{-1} in the 700–4000 cm^{-1} spectral range. The solid samples were

Table 1 General information for the Hassi-Messaoud well and storage tank oils

	Hassi-Messaoud well oil	Stock tank oil
Gravity, °API	45	42
Viscosity, cp 40°	2.23	1.5
Asphaltene, % w/w	0.70	0.15
Resin, % w/w	24.5	13.3
Total acidity, mg-KOH/g	0.96	–

introduced directly in ATR top plates which have composite zinc selenide (ZnSe) and diamond crystals.

^{1}H-NMR spectra were obtained from a 250 MHz spectrometer (Bruker 250) with pulse width of 3.5 µs (30° flip angle), recycle delay of 2 s at least 600 scans, tube diameter 5 mm, and spectral width of 18 ppm. Chemical shifts (δ) are reported relative to tetramethylsilane (TMS) used as an internal standard and the spectra were recorded in deuterated-dichloromethane (CD_2Cl_2).

The samples prepared by dissolution in toluene at a concentration of 5 mg L^{-1} were examined by emission fluorescence spectroscopy (Fluoromax-3) in the range from 350 to 700 nm with an excitation wavelength of 256 nm.

Carbon, hydrogen, nitrogen, and sulfur contents of asphaltene fractions were determined using a Thermo Finnigan EA 1112 elemental analyzer. Experimental accuracy of these measurements was 0.2 %.

With ^{1}H-NMR and elemental analysis measurements, the aromaticity factor (f_a), the average number of carbons per alkyl side chain (n), and shape factor of the aromatic sheet (Φ) of both asphaltene fractions were evaluated with the formulae reported in the literature (Dickinson 1980; Daaou et al. 2008, 2009; Matsumura and Sato 2009).

Surface tensions of asphaltenes solutions (0.05–10 g L^{-1}) in toluene, pyridine, or nitrobenzene were measured with a Cochon–Abrie tensiometer employing the Wilhelmy plate method. All the measurements were conducted in a temperature-controlled cell at 20 ± 0.1 °C, and each measure was repeated three times. The maximum error in these measurements was 0.1 mN m^{-1}.

3 Results and discussion

3.1 Structural characterization

The differences in the average chemical structures of the asphaltene molecules separated from the storage tank deposit, $(AS)_{DP}$ and the petroleum well, $(AS)_{WL}$ were studied using elemental analysis, FTIR, fluorescence spectroscopy, and proton nuclear magnetic resonance (^{1}H-NMR).

Results of C, H, N, S, and O (determined by difference) analysis of asphaltene fractions given in Table 2 showed a

Table 2 Elemental composition and corresponding atoms to carbon ratio of the asphaltenes samples

%wt	$(AS)_{DP}$	$(AS)_{WL}$
C	79.2	84.3
H	8.2	7.5
N	0.8	0.7
S	3.1	0.4
O[a]	8.7	7.1
E[b]	12.6	8.2
H/C	1.24	1.07
O/C	0.082	0.063
N/C	0.008	0.007
S/C	0.015	0.002
E/C	0.105	0.072

[a] Determined by difference

[b] Total heteroatoms ($E = O + S + N$)

much higher content of heteroatoms, especially of oxygen and sulfur, in the asphaltenes extracted from the storage tank deposit $(AS)_{DP}$, suggesting that this fraction is more polar than $(AS)_{WL}$. In fact, the S/C and O/C ratio values are 6.0 and 1.7 times, respectively, higher in $(AS)_{DP}$. A small difference in N/C ratio between $(AS)_{DP}$ and $(AS)_{WL}$ was also observed. The greater value of H/C ratio observed for $(AS)_{DP}$ fraction indicates that this fraction is less aromatic than $(AS)_{WL}$.

The FTIR spectra of both the asphaltene fractions (Fig. 1) are very similar to the spectra of other asphaltenes published in the literature (Calemma et al. 1995; Ascanius et al. 2004; Daaou et al. 2008). The FTIR band assignment for asphaltene samples is summarized in Table 3. The spectra show peaks at 2935/1460 and 2850/1370 cm^{-1} which correspond to CH$_3$ and CH$_2$ aliphatic groups. The aromatic C=C and C=O (ketones, aldehydes, or carboxylic acids) bands are observed at around 1600 and at 1708 cm^{-1}, respectively. Particularly, the $(AS)_{DP}$ spectra display three peaks at 1770 and 1260/1150 cm^{-1} which are related to the presence of C=O and C–O of ester groups, respectively. A distinct band in the range between 3500 and 3100 cm^{-1} is also observed for $(AS)_{DP}$, indicating the presence of N–H and O–H groups.

In conclusion, these results are in agreement with those obtained by elemental analysis and justify the higher polarity of the $(AS)_{DP}$ fraction.
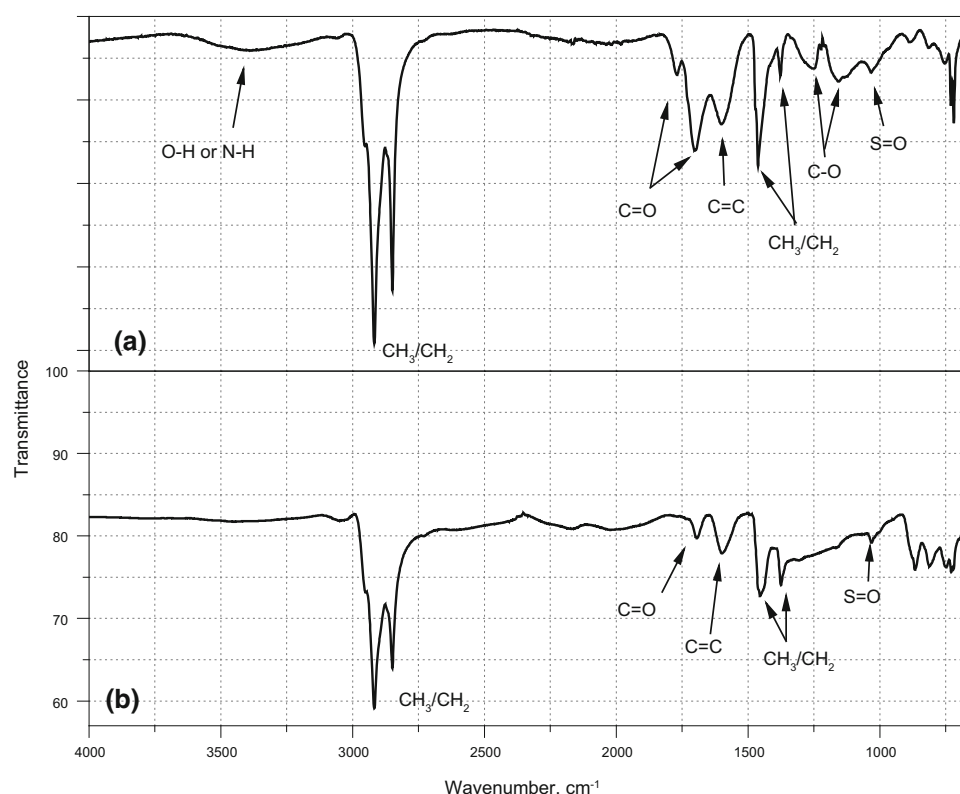
Fig. 1 FTIR spectrum of **a** AS$_{DP}$ and **b** AS$_{WL}$ asphaltenes

Table 3 Infrared spectral range assignments for asphaltene samples: strong (s), medium (m), weak (w)

Absorption frequency, cm^{-1}	Functional group	Asphaltenes characteristic bands	
		(AS)$_{DP}$	(AS)$_{WL}$
3100–3500	O–H or N–H (stretching)	3393 (w)	–
2800–3000	C–H (stretching)	2920 (s), 2850 (s)	2915 (s), 2845 (s)
1600–1800	C=O	1708 (m), 1770 (w)	1702 (w)
1590–1620	C=C (aromatic stretching)	1603 (m)	1595 (m)
1375–1450	(C–H deformation)	1460 (s), 1373 (s)	1450 (s), 1373 (s)
1300–1050	C–O of esters	1260/1150	–
∼1000	S=O	1032 (w)	1030 (w)

For further interpretation of these results, the areas under the aliphatic stretching absorption in the range 3000–2770 cm^{-1} (A_1), the carbonyl stretching absorption in the range 1750–1650 cm^{-1} [for (AS)$_{WL}$] and in the range 1750–1650 and 1790–1750 cm^{-1} [for (AS)$_{DP}$] (A_2), and the aromatic C=C stretching vibrations in the range 1650–1520 cm^{-1} (A_3) were integrated. From these, two ratios A_3/A_1 and A_2/A_3 are evaluated and reported in Table 4. The first ratio is a measure indicating the degree of aromaticity in the molecular matrix and the second one representing the degree of carbonyl concentration per unit aromatic structure. From the results of these two ratios, it can be revealed that the (AS)$_{WL}$ asphaltene is more aromatic and less polar than (AS)$_{DP}$ sample.

Fluorescence emission spectra of asphaltenes samples presented in Fig. 2 are similar to those found in the literature (Ralston et al. 1996; Groenzin and Mullins 1999; Badre et al. 2006). The peak location exhibits a shift that can be explained in terms of the aromatic rings number and of the condensation rate of the polyaromatic structure. Indeed, the emission at shorter wavelength (λ_{em}) would, in principle, imply the presence of smaller aromatic rings (Ralston et al. 1996), while the displacement of the bands to longer λ_{em} (red shift) (Pesce et al. 1971) can correspond to larger aromatic rings. The comparison between the asphaltene samples' emission spectra shows that the (AS)$_{WL}$ spectrum is shifted to greater value of λ_{em} value (490 nm) with respect to (AS)$_{DP}$ (455 nm). This indicates

Table 4 Areas under aliphatic (A_1), carbonyl (A_2), and aromatic (A_3) bands determined from FTIR spectra and corresponding aromatic (A_3/A_1) and carbonyl (A_2/A_3) indexes for the both asphaltenes samples

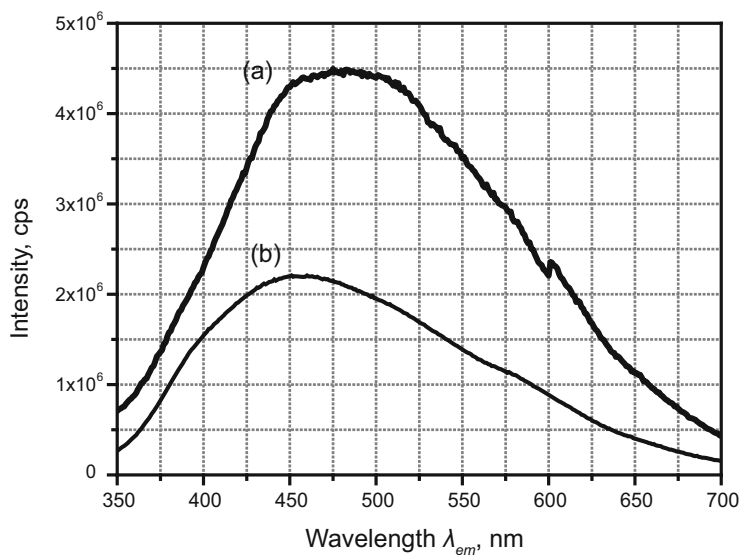| Area	A_1 3000–2770, cm^{-1}	A_2 1790–1750, cm^{-1} and/or 1750–1650, cm^{-1}	A_3 1650–1520, cm^{-1}	A_3/A_1	A_2/A_3
$(AS)_{DP}$	275	188	136	0.49	1.39
$(AS)_{WL}$	272	124	160	0.59	0.77

Fig. 2 Fluorescence spectrum in emission mode of **a** $(AS)_{DP}$, and **b** $(AS)_{WL}$ asphaltenes at $\lambda_{ex} = 265$ nm

that the two investigated asphaltene fractions were different in aromatic hydrocarbon ring number and in the aromatic ring arrangement. The analysis of the present results in terms of the literature data of the shortest emission wavelength of a series of polyaromatic compounds (Badre et al. 2006) suggests that the $(AS)_{DP}$ and $(AS)_{WL}$ asphaltene samples contain 3–4 and 5–6 fused aromatic rings, respectively.

^{1}H-NMR spectra presented in Fig. 3 show four signals observed at 0–1.0, 1.0–2.0, 2.0–4.0, and 6.5–9.0 ppm and corresponding, respectively, to aliphatic protons in γ (H_γ), β (H_β), and α (H_α) positions to aromatic ring and aromatic protons (H_{ar}). The atomic abundances of each proton type obtained from their corresponding integrated band areas are reported in Table 5. From these results together with the elemental analysis data (Table 2), the main molecular parameters of asphaltene fractions, such as aromaticity factor (f_a), alkyl side chain (n), and shape factor of the aromatic sheet, (Φ) are calculated according to the formulas proposed by Speight (Speight 1970).

$$f_a = \frac{c_A}{c_T} = 1 - \left(\frac{H}{c}\right)\left(\frac{H_\alpha + H_\beta}{2} + \frac{H_\gamma}{3}\right) \tag{1}$$

$$\phi = \frac{c_A}{c_T} = \frac{\left(H_{ar} + \frac{H_\alpha}{2}\right)}{\left(\frac{H}{c}\right)\left(\frac{H_\alpha + H_\beta}{2} + \frac{H_\gamma}{3}\right)} \tag{2}$$

$$n = \frac{H_\alpha + H_\beta + H_\gamma}{H} \tag{3}$$

where C_A, C_T, and C_p are the aromatic, the total, and the peripheral condensed aromatic carbons numbers, respectively. H_α, H_β, and H_γ are the percentages of the aliphatic protons in α, β, and γ positions obtained as the corresponding ratio of the ^{1}H-NMR spectrum integration area to the total integration area of the ^{1}H-NMR spectrum. H_{ar} is the ratio of the ^{1}H NMR spectrum integration area of the aromatic proton to the total integration area of the ^{1}H NMR spectrum.

The H_α, H_β, H_γ, and H_{ar} percentages and the average structural parameter results of both asphaltene fractions are given in Table 5. The results show a notable difference in both aromatic sheet shape and aromaticity factors for $(AS)_{DP}$ and $(AS)_{WL}$. The latter sample has the higher aromaticity ($f_a = 0.53$) and the smaller aromatic sheet shape factors ($\Phi = 0.35$) in comparison with $(AS)_{DP}$ ($f_a = 0.43$ and $\Phi = 0.55$). The smaller aromatic sheet shape factor value can indicate that the aromatic rings are very condensed in $(AS)_{WL}$ molecules with respect to $(AS)_{DP}$. These results agree with the conclusions drawn from elemental analysis (H/C), FTIR (A_3/A_1), and fluorescence (λ_{em}) measurements. The alkyl side chain is relatively long for $(AS)_{DP}$ asphaltenes.
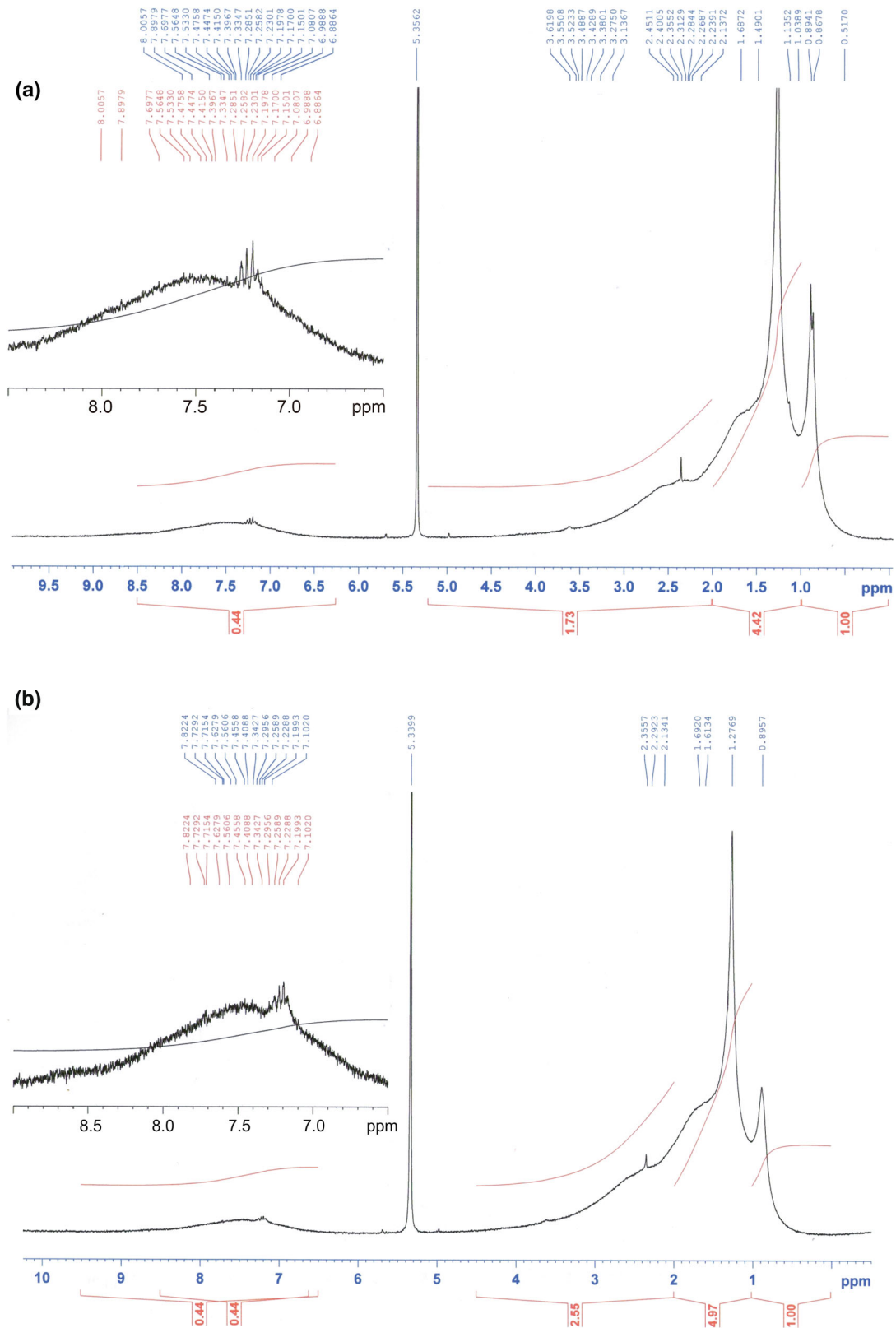
Fig. 3 Liquid state ^1H NMR spectrum of **a** AS_{DP} and **b** AS_{WL} asphaltenes

Table 5 Assignments of proton chemical shift NMR spectra and average molecular parameters of $(AS)_{DP}$ and $(AS)_{WL}$ asphaltenes molecules calculated from the correlation Eqs. (1)–(3)

%wt	$(AS)_{DP}$	$(AS)_{WL}$
H_α	28.46	22.79
H_β	55.47	58.23
H_γ	11.16	13.20
H_{ar}	04.91	05.60
H_{al}	95.09	94.40
f_a	0.43	0.53
Φ	0.55	0.35
n	3.34	4.10

Speight (1970)

3.2 Surface tension

Results of the surface tension measurements of $(AS)_{DP}$ and $(AS)_{WL}$ solutions in toluene, pyridine, and nitrobenzene are plotted in Fig. 4a, b, respectively. The variation of surface tension is small as already observed by other authors for various asphaltenes (Bardon et al. 1996; Sheu 1996). Upon increase of asphaltene concentration, surface tension curves showed distinct discontinuities similar to those observed in surfactant solutions, and with this in mind, these discontinuities were considered as an indication of the occurrence of an aggregation phenomenon, in accordance with the Gibbs equation and defined a CMC for asphaltenes in each solvent (Loh et al. 1999; Mohamed et al. 1999). It was established that this parameter (CMC) is an indicator of asphaltene molecule association. Indeed, below the CMC value, the asphaltenes are in a molecular state, while above CMC, associated asphaltenes are formed (Priyanto et al. 2001). The CMC values are given in Table 6 and indicate that for each asphaltene sample, the CMC value increases with increasing solvents' solubility parameter and polarity. Indeed, in a more polar solvent, nitrobenzene (21.8 MPa$^{1/2}$), both $(AS)_{DP}$ and $(AS)_{WL}$ can form micelles in higher concentration than in a less polar solvent, toluene (18.5 MPa$^{1/2}$). These results are in good agreement with those found by Rogel et al. (2000) and Kyeongseok et al. (2004). Comparison of the studied asphaltenic fractions shows that $(AS)_{WL}$ is more soluble in toluene than $(AS)_{DP}$, but less soluble in nitrobenzene. This can be explained in terms of
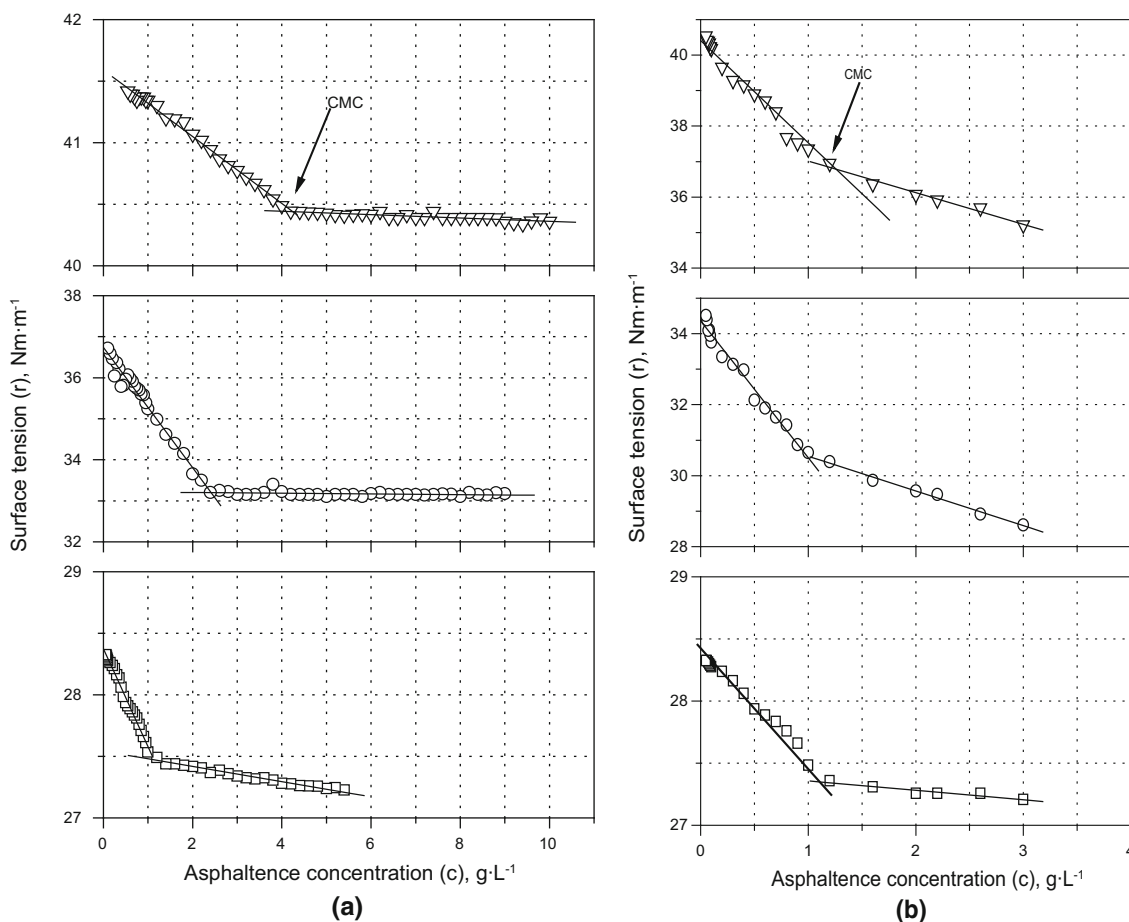

Fig. 4 Surface tension as a function of concentration in g L^{-1} for **a** AS$_{DP}$ and **b** AS$_{WL}$ asphaltenes in nitrobenzene (*inverted triangle*), pyridine (*circle*), and toluene (*square*). Full lines correspond to the linear fit

Table 6 CMC (g L^{-1}) and molecular areas A_a (Å^2) values of asphaltenes samples in different solvents

Asphaltenes	Toluene		Nitrobenzene		Pyridine	
	CMC, g L^{-1}	A_a, Å^2	CMC, g L^{-1}	A_a, Å^2	CMC, g L^{-1}	A_a, Å^2
(AS)$_{WL}$	1.10	774	1.31	175	1.06	166
(AS)$_{DP}$	0.98	434	4.17	489	2.36	177

structure parameters determined above. In fact, the more polar asphaltene with a lower aromaticity, (AS)$_{DP}$, corresponds to the higher solubility in a polar solvent (nitrobenzene). The less polar and higher aromaticity one, (AS)$_{WL}$, is more soluble in solvent with low polarity (toluene). These results indicate that the association of more polar and less aromatic asphaltene (AS)$_{DP}$ is probably dominated by strong specific polar and hydrogen-bonding forces (Porte et al. 2003) rather than other interactions like as π–π bonding of aromatic rings and Van der Waals interactions of long-chain hydrocarbons (Spiecker et al. 2003). These findings confirm suggestions of Rogel et al. (2000) and indicate that the self-aggregation behavior is related to the structural and compositional characteristics. Moreover, the same properties determine the solubility parameters of asphaltenes, and as a consequence, their solubility behavior. The content and the nature of heteroatoms influence the polarity of asphaltenes. Higher polarity favors association and self-assembly. Therefore, asphaltenes with a higher content of heteroatoms such as O, N, and S display a higher degree of self-assembling depending on the polarity of the surrounding medium. The molecular area of the asphaltene (A_a) adsorbed to the liquid surface may be calculated using the Gibbs Eq. (4):

$$A_a = \frac{1}{N_A \Gamma} \qquad (4)$$

where N_A is Avogadro's number and Γ is the surface concentration of the adsorbed species and can be obtained from the curve by evaluating the slope just below the CMC, using the Gibbs equation (Sheu 1996).

Results presented in Table 6 show the molecular area, A_a, of both asphaltenes (AS)$_{DP}$ and (AS)$_{WL}$ in different solvents. The values obtained vary in the range 165–774 Å^2. It may be noticed that A_a of (AS)$_{DP}$ is higher than that obtained for (AS)$_{WL}$ in polar solvents such as pyridine and nitrobenzene. In a non-polar solvent-like toluene, the situation is reversed. Thus, the polarities of the solvent and of asphaltenes determine the arrangement of asphaltene molecules at the surface.

4 Conclusion

Two asphaltenes samples derived from different sources of Algerian petroleum have been characterized to compare their structure and aggregation behaviors in the presence of three solvents (toluene, pyridine, and nitrobenzene) with different solubility parameters and polarities.

Elemental analysis, FTIR, ^{1}H-NMR, and fluorescence spectroscopy methods indicate that there is a notable difference between their structures. This difference appears principally in both aromaticity and polarity (heteroatoms content) properties. The unstable asphaltenes (AS)$_{DP}$, which were extracted from the stage tank deposit, have a higher heteroatoms content ($E = 12.6$ wt%), lower aromaticity factor ($f_a = 0.43$), and higher aromatic sheet shape factor ($\Phi = 0.55$) in comparison with the stable sample derived directly from the petroleum well (AS)$_{WL}$ ($E = 8.2$ wt%, $f_a = 0.53$, and $\Phi = 0.35$). The alkyl side chain is relatively long for (AS)$_{DP}$ asphaltenes ($n = 4$). These results confirm, as already suggested, that asphaltene instability is principally governed by both aromaticity and polarity properties.

The surface tension method allowed investigation of the asphaltenes aggregation. It was found that the CMC and corresponding molecular areas values ranged from 0.98 to 4.17 g L^{-1} and 166 to 775 Å^2, respectively. It may be concluded that the aggregation behavior is governed by asphaltene structure and polarity as well as by the polarity of the solvent. Indeed, the more polar the solvent, the higher is the CMC with both (AS)$_{DP}$ and (AS)$_{WL}$ fractions. Consequently, it was found that the more polar asphaltene with a lower aromaticity, (AS)$_{DP}$ displays the higher solubility and the higher specific area at the surface in a polar solvent (nitrobenzene). (AS)$_{WL}$ asphaltenes that are less polar and display a higher aromaticity can form aggregates at lower concentrations (low CMC) in a non-polar solvent (toluene) and display a lower specific area at the surface.

These results confirm the recommendations of Rogel et al. (2000) and indicate that the self-aggregation behavior is related to the structural and compositional characteristics (polarity and aromaticity) which determine their solubility parameters, and as a consequence, their solubility behavior.

References

Acevedo S, Gutierrez LB, Negrin G, Pereira JC, Delolme BMF, Dessalces G, Broseta D. Molecular weight of petroleum asphaltenes: a comparison between mass spectrometry and vapor pressure osmometry. Energy Fuels. 2005;19:1548–60.

Ancheyta J, Centeno G, Trejo F, et al. Extraction and characterization of asphaltenes from different crude oils and solvents. Energy Fuels. 2002;16:1121–7.

Andersen SI, Christensen SD. The critical micelle concentration of asphaltenes as measured by calorimetry. Energy Fuels. 2000;14:38–42.

Andersen SI, Bridi KS. Aggregation of asphaltenes as determined by calorimetry. J Colloid Interface Sci. 1991;142:497–502.

Ascanius BE, Garcia DM, Andersen SI. Analysis of asphaltenes subfractionated by n-methyl-2-pyrrolidone. Energy Fuels. 2004;18:1827–31.

Avid B, Sato S, Takanohashi T, et al. Characterization of asphaltenes from Brazilian vacuum residue using heptane-toluene mixtures. Energy Fuels. 2004;18:1792–7.

Badre S, Goncalves CC, Norinaga K, et al. Molecular size and weight of asphaltene and asphaltene solubility fractions from coals crude oils and bitumen. Fuel. 2006;85:1–11.

Bardon C, Barré L, Espinat D, et al. The colloidal structure of crude oils and suspensions of asphaltenes and resins. Fuel Sci Technol Int. 1996;14:203–42.

Bouhadda Y, Bendedouch D, Sheu E, et al. Some preliminary results on a physico-chemical characterization of a Hassi Messaoud petroleum asphaltene. Energy Fuels. 2000;14:845–53.

Buenrostro-Gonzalez E, Andersen SI, Garcia-Martinez JA, et al. Solubility/molecular structure relationships of asphaltenes in polar and nonpolar media. Energy Fuels. 2002;16:732–41.

Calemma V, Iwanski P, Nali M, et al. Structural characterization of asphaltenes of different origins. Energy Fuels. 1995;9:225–30.

Carbognani L, Espidel J, Izquierdo A. In: Yen TF, Chilingarian GV, editors. Asphaltenes and asphalts: developments in petroleum science. Amsterdam: Elsevier; 1997 (chapter 13).

Daaou M, Bendedouch D, Bouhadda Y, et al. Explaining the flocculation of Hassi Messaoud asphaltenes in terms of structural characteristics of monomers and aggregates. Energy Fuels. 2009;23:5556–63.

Daaou M, Modarressi A, Bendedouch D, et al. Characterization of the non-stable fraction of Hassi-Messaoud asphaltenes. Energy Fuels. 2008;22:3134–41.

Da Silva Ramos AC, Haraguchi L, Nostripe FR, et al. Interfacial and colloidal behavior of asphaltenes obtained from Brazilian crude oils. J Pet Sci Eng. 2001;32:201–16.

Dereppe JM, Moreaux C, Castex H. Analysis of asphaltenes by carbon and proton nuclear magnetic resonance spectroscopy. Fuel. 1978;57:435–41.

Dickinson EM. Structural comparison of petroleum fractions using proton and 13C-NMR spectroscopy. Fuel. 1980;59:290–4.

Groenzin H, Mullins OC. Petroleum asphaltene molecular size and structure. J Phys Chem A. 1999;103:11237–45.

Groenzin H, Mullins OC. Molecular size and structure of asphaltenes from various sources. Energy Fuels. 2000;14:677–84.

Ibrahim YA, Abdelhameed MA, Al-sahhaf TA, et al. Structural characterization of different asphaltenes of Kuwaiti origin. Pet Sci Technol. 2003;21:825–37.

Khan MA, Ahmed I, Ishaq M, et al. Spectral characterization of liquefied products of Pakistani coal. Fuel Process Technol. 2003;85:63–74.

Kokal SL, Sayegh SG. Asphaltenes: the cholesterol of petroleum. March, 1995, Presented at the SPE Middle East Oil Show; Society of Petroleum Engineers: Bahrain; SPE 29787.

Kyeongseok O, Terry AR, Milind DD. Asphaltene aggregation in organic solvents. J Colloid Interface Sci. 2004;271:212–9.

Loh W, Mohamed RS, Ramos AC. Aggregation of asphaltenes obtained from a Brazilian crude oil in aromatic solvents. Pet Sci Technol. 1999;17:147–63.

Matsumura A, Sato S. Estimation of carbon aromaticity for asphaltenes by elemental analysis and proton NMR. Journal of the Japan Institute of Energy. 2009;88:586–91.

Mohamed RS, Ramos ACS, Loh W. Aggregation Behavior of two asphaltenic fractions in aromatic solvents. Energy Fuels. 1999;13:323–7.

Mullins OC. Asphaltenes in crude oil: absorbers and/or scatterers in the near-infrared region? Anal Chem. 1990;62(5):508–14.

Murgich J, Rodriguez J, Aray Y. Molecular recognition and molecular mechanics of micelles of some model asphaltenes and resins. Energy Fuels. 1996;10:68–76.

Murgich J. Intermolecular forces in aggregates of asphaltenes and resins. Pet Sci Technol. 2002;20:983–97.

Pekerar S, Lehmann T, Mendez B, et al. Mobility of Asphaltene samples studied by 13C NMR spectroscopy. Energy Fuels. 1999;13:305–8.

Pesce AJ, Rosen CG, Pasby TL. Fluorescence spectroscopy. New York: Marcel Dekker; 1971. p. 54.

Porte G, Zhou H, Lazzeri V. Reversible description of asphaltene colloidal association and precipitation. Langmuir. 2003;19:40–7.

Priyanto S, Ali Mansoori G, Suwono A. Measurement of property relationships of nano-structure micelles and coacervates of asphaltene in a pure solvent. Chem Eng Sci. 2001;56:6933–9.

Ralston CY, Kirtley SM, Mullins OC. Small population of one to three fused-aromatic ring moieties in asphaltenes. Energy Fuels. 1996;10:623–30.

Rogel E, Leon O, Torres G, Espidel J. Aggregation of asphaltenes in organic solvents using surface tension measurements. Fuel. 2000;79:1389–94.

Sheu EY, Storm DA. Colloidal properties of asphaltenes in organic systems. In: Sheu EY, Mullins OC, editors. Asphaltenes: fundamentals and applications. New York: Plenum Press; 1995. p. 1.

Sheu EY. Physics of asphaltene micelles and microemulsions—theory and experiment. J Phys: Condens Matter. 1996;8:A125.

Shirokoff JW, Siddiqui MN, Ali MF. Characterization of the structure of Saudi Crude asphaltenes by X-ray diffraction. Energy Fuels. 1997;11:561–5.

Siskin M, Kelemen SR, Eppig CP, et al. Asphaltene molecular structure and chemical influences on the morphology of coke produced in delayed coking. Energy Fuels. 2006;20:1227–34.

Speight JG. A structural investigation of the constituents of Athabasca bitumen by proton magnetic resonance spectroscopy. Fuel. 1970;49:76–90.

Spiecker PM, Gawrys KL, Kilpatrick PK. Aggregation and solubility behavior of asphaltenes and their subfractions. J Colloid Interface Sci. 2003;267:178–93.

Storm DA, Barresi RJ, De Canio SJ. Colloidal nature of vacuum residue. Fuel. 1991;70:779–82.

Taylor SE. Use of surface tension measurements to evaluate aggregation of asphaltenes in organic solvents. Fuel. 1992;71:1338–9.

Yang X, Hamza H, Czarnecki J. Investigation of subfractions of Athabasca asphaltenes and their role in emulsion stability. Energy Fuels. 2004;18:770–7.

Yarranton HW, Alboudwarej H, Jakher R. Investigation of asphaltene association with vapor pressure osmometry and interfacial tension measurements. Ind Eng Chem Res. 2000;39:2916–24.